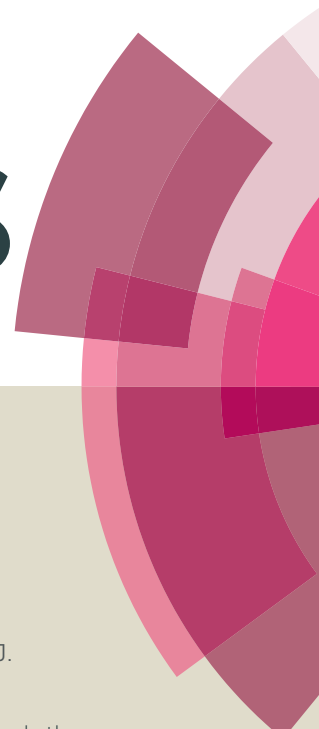


RSC Advances



This article can be cited before page numbers have been issued, to do this please use: G. Pan, S. Fan, J. Liang, Y. Liu and Z. Tian, *RSC Adv.*, 2015, DOI: 10.1039/C5RA05635G.



This is an *Accepted Manuscript*, which has been through the Royal Society of Chemistry peer review process and has been accepted for publication.

Accepted Manuscripts are published online shortly after acceptance, before technical editing, formatting and proof reading. Using this free service, authors can make their results available to the community, in citable form, before we publish the edited article. This *Accepted Manuscript* will be replaced by the edited, formatted and paginated article as soon as this is available.

You can find more information about *Accepted Manuscripts* in the [Information for Authors](#).

Please note that technical editing may introduce minor changes to the text and/or graphics, which may alter content. The journal's standard [Terms & Conditions](#) and the [Ethical guidelines](#) still apply. In no event shall the Royal Society of Chemistry be held responsible for any errors or omissions in this *Accepted Manuscript* or any consequences arising from the use of any information it contains.

CVD synthesis of Cu₂O films for catalytic application

Guan-Fu Pan,^{a,b} Shi-Bin Fan,^{a,b} Jing Liang,^{a,c} Yue-Xi Liu^{a,b} and Zhen-Yu Tian^{a,*}

Received 00th January 20xx,
Accepted 00th January 20xx

DOI: 10.1039/x0xx00000x

www.rsc.org/

Pure Cu₂O was synthesized at 270 °C by pulsed-spray evaporation chemical vapor deposition. The results indicate that Cu₂O is effective for the complete oxidation of VOCs with good reusability and reproducibility. The lattice and adsorbed oxygen as well as the hollow ball-like geometry are dedicated to the catalytic processes.

1. Introduction

Volatile organic compounds (VOCs) are the main air pollutants emitted from the combustion of fossil fuels in many industry processes and transportation activities.^{1,2} VOCs are associated with various health-related problems.³ Catalytic combustion was commonly used for the abatement of VOCs in the past decades.⁴ The involved catalysts are mainly composed of noble metals such as Au, Pt and Rh⁵⁻⁷ and transition metal oxides (TMOs).^{8,9} Noble metals generally exhibit good catalytic performance, but they are expensive and easy to be poisoned. For these reasons, catalytic oxidation of VOCs over TMOs has captured increasing attention, and considerable efforts have been devoted to the synthesis and application of TMOs for such purposes.¹⁰ Specifically, Mn₃O₄, CuO, Fe₂O₃ and Co₃O₄ exhibited good performance as active catalysts for VOCs treatment.^{4,11-14}

Compared to other TMOs, Cu₂O has excellent catalytic applications for VOCs.¹⁵ Rostami and Jafari¹⁶ used Cu₂O as an efficient catalyst to remove aromatic compounds. Kim and Shim¹⁵ investigated the catalytic characteristic of Cu₂O and concluded that Cu₂O was active for the removal of VOCs.

Several methods were involved in the production of Cu₂O, such as sol-gel,¹⁷ top-down approach with nanosecond and picosecond lasers,¹⁸ honey aided solution synthesis,¹⁹ electrochemical synthesis²⁰ and photonic crystal template-assisted electrodeposition.²¹ However, a mixture of Cu, Cu₂O and CuO was

generally obtained by those methods and synthesis of pure Cu₂O was scarce. In recent years, pulsed-spray evaporation chemical vapor deposition (PSE-CVD) has been successfully used to prepare a series of TMOs, e.g., Co₃O₄²² and Mn₃O₄.²³ Compared to the above-mentioned techniques, PSE-CVD is easy to control the thickness and quality of the films without any further treatment. Thus, PSE-CVD exhibits great potential to prepare Cu₂O thin films.

In the current work, the Cu₂O thin films were synthesized by a home-made PSE-CVD system. Among the VOCs, unsaturated hydrocarbons are often encountered emissions from hydrocarbon flames. Since the unsaturated hydrocarbons such as C₂H₂ and C₃H₆ are quite difficult to be oxidized, especially C₂H₂ is an important precursor to form soot during the combustion of fossil fuel, C₂H₂ and C₃H₆ were selected as representatives for the deep oxidation of VOCs existed in the exhaust emissions. The prepared Cu₂O samples were characterized in terms of structure, morphology and composition as well as catalytic performance.

2. Material and methods

2.1 Preparation of Cu₂O thin films

The Cu₂O thin films were synthesized in a PSE-CVD system combined with cold-wall stagnation point-flow CVD reactor and waste collector, as presented in Fig. 1. The preparation process consists of four steps. Firstly, copper acetylacetonate (Cu(acac)₂) was dissolved in ethanol at a concentration of 2.5 mM, which was delivered as liquid feedstock by a PSE unit. The delivery frequency was 4 Hz and the opening time of PSE was 2.5 ms. The feeding rate was 1.03 mL/min. The 30 cm long evaporation chamber was kept at 3.0 kPa and 180 °C. Secondly, the resulting vapor was transported into the deposition chamber with O₂ and N₂ with flowrates of 1.0 and 0.5 standard liter per minute (SLM), respectively. Thirdly, the Cu₂O thin films were formed on different substrates (planar glass, stainless steel and mesh grid) kept at 270 °C for characterization purposes. Finally, the waste vapor was collected by a liquid nitrogen trap. The details of the optimized conditions are summarized in Table ESI S1.

2.2 Characterization

The obtained Cu₂O films were characterized in terms of structure, morphology and chemical composition with X-ray diffraction

^aInstitute of Engineering Thermophysics, Chinese Academy of Sciences, 11 Beisihuanxi Road, Beijing 100190, China.

^bUniversity of Chinese Academy of Sciences, Beijing 100049, China.

^cSchool of Energy, Power and Mechanical Engineering, North China Electric Power University, Beijing 102206, China.

† Electronic Supplementary Information (ESI) available: experimental conditions, some XPS spectra and outlet profiles of CO and CO₂ during the catalytic tests. See DOI: 10.1039/x0xx00000x

(XRD), Scanning electron microscopy (SEM) and X-ray photoelectron spectroscopy (XPS), respectively. XRD analysis was performed on Bruker D8 Focus with Cu K α radiation, scan angle of 5–90° and scanning step of 0.02°. The microstructure was examined using SEM (S-4800 Hitachi) with the resolution of 1.5 nm (15 KV). The chemical composition was identified by the XPS (ESCALAB 250Xi) with pass energy of 20 eV and energy step size of 0.050 eV. The XPS results were analyzed by Avantage which is one of the most widely used softwares for XPS analysis. The elemental contents in the samples was quantitative analyzed by non-linear least square fitting method and the oxygen was analyzed by Unimodal fitting method.²⁴

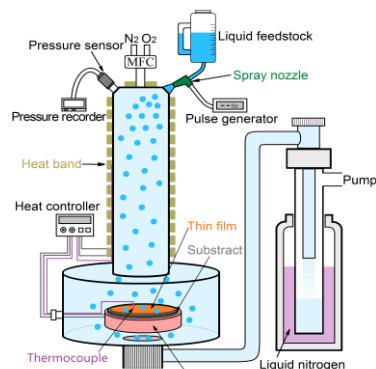


Fig. 1 Schematic diagram of the PSE-CVD system.

2.3 Catalytic test

The performances of the Cu₂O films for C₂H₂ and C₃H₆ conversion were investigated by a fixed bed quartz reactor, as shown in Fig. 2. A 60 cm long alundum tube (8.0 mm inner diameter) was fixed in a digital electrical furnace. 20 mg of the Cu₂O supported on grid mesh of stainless steel was located at the isothermal area. A K-thermocouple was used to measure the temperature of Cu₂O film. A gas mixture consisted of 1 % fuel gas (C₂H₂ or C₃H₆), 10 % O₂ and 89 % Ar was introduced into the alundum tube with a total flow rate of 15 ml/min, corresponding to the gaseous hourly space velocity (ghsv) of 45,000 ml g⁻¹ cat h⁻¹. The temperature of the furnace was risen with a ramp of 2 °C/min. Finally, the exhausting gas was measured by a gas chromatograph (Agilent, GC3000) for qualitative and quantitative analysis.

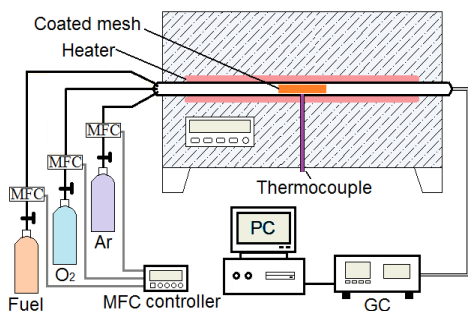


Fig. 2 Experimental setup of catalytic test.

3. Results and discussion

3.1 Growth

By measuring the weight difference of the substrates before and after deposition, the growth of the prepared films can be estimated. As displayed in Fig. 3, a linear behavior is observed and the growth

rate of Cu₂O is calculated to be 1.6 nm/min. According to Tian et al.,²⁵ the increase of the pressure may promote full surface coverage by adsorbing more Cu(acac)₂ and O₂, which could accelerate the nucleation step and result in a high growth rate. In this work, the pressure for the synthesis of Cu₂O films was optimized to be 3.0 kPa. According to the previous results,²⁵ the substrate temperature should be lower than 275 °C for the synthesis of pure Cu₂O. In the experiments, the temperature for the synthesis of Cu₂O was fixed at 270 °C. Similar to the same strategy,²⁵ the other parameters such as the concentration of the precursor in the liquid feedstock, the pulse width and frequency of the precursor delivery have also been optimized (see Table ESI S1). The results also indicate that the synthesis of Cu₂O with PSE-CVD system can be tailored with respect to thickness.

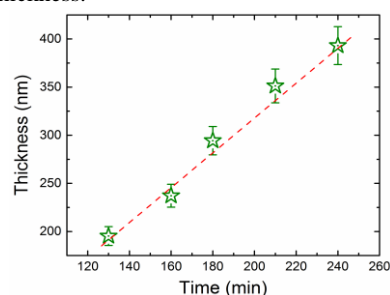


Fig. 3 Linear growth of Cu₂O thin films on stainless steel.

3.2 Phase identification

The XRD pattern of the obtained thin film is shown in Fig. 4. The well-defined diffraction peaks are observed at 36.41°, 42.24°, and 61.88°, which can be well attributed to (111), (200) and (220) orientations of Cu₂O in the literature (JCPDS Nr. 05-0667). The two weak peaks located at 29.73° and 73.81° fit well with the (110) and (311) planes of Cu₂O. No characteristic peaks of any other impurities were observed in the XRD patterns, indicating the formation of monoclinic Cu₂O phase.^{26, 27} In the work by Medina Valtierra et al.,²⁶ they prepared Cu₂O film by CVD with the same precursor. However, no film of Cu₂O was formed when the deposition temperature was lower than 320 °C. For sample prepared at 320 °C, only (111) and (200) planes were observed.²⁶ However, the XRD analysis indicates that pure Cu₂O thin films can be easily prepared by PSE-CVD at as low as 270 °C in this work.

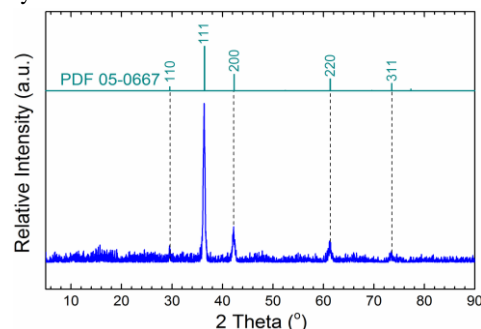


Fig. 4 XRD pattern of the Cu₂O thin film prepared on glass at 270 °C.

3.3 Microstructural studies

The sharp and strong reflection peaks suggest that the prepared samples are well crystallized. The crystallite size and the micro-strain of Cu₂O thin films were calculated to be 29 nm and 0.06% by applying Scherrer's formula: $D = 0.9\lambda/\beta \cos \theta$ and the equation $\epsilon = \beta/2\cot\theta$ to the most intense diffraction peak, where $\lambda =$

0.154056 nm, β and θ represent the full width at half maximum and diffraction angle of the observed peak, respectively.²⁸

The formation of Cu₂O can be preceded with the adsorption of the precursor on the heated substrate, ligands removal, formation of Cu metal and oxidation of Cu to Cu₂O. Both temperature and pressure play important roles in the deposition processes. With the same precursor, a pure phase of CuO phase was obtained at 300 °C by Tian et al.,²⁵ while Cu₂O was formed at 320 °C by Medina-Valtierra et al.²⁶ Such high temperature for Cu₂O formation could be due to the usage of low flowrate of O₂ flow (30 ml/min) in their work.

SEM inspection was carried out to reveal the morphology of the as-obtained Cu₂O samples. The representative SEM images with different magnifications are shown in Fig. 5. The SEM images indicate that the film is homogeneous and is composed of a large quantity of small ball-like particles. The average grain size is estimated to be 30 nm, which matches well with the crystallite size calculated by the XRD results. The calculated size is much smaller than that prepared with electrodeposition (500-700 nm) by Yu et al.²⁹ Besides the ball-like shapes, a number of hollows are also observed. The small grain size and hollows could absorb more oxygen than the smooth surface, which would benefit for the catalytic oxidation of VOCs.

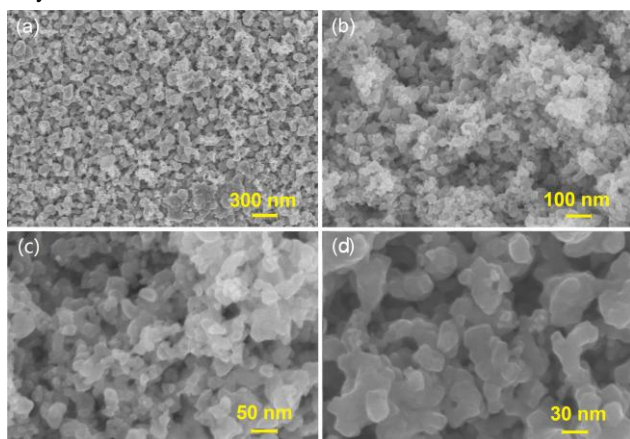


Fig. 5 SEM images of thin Cu₂O films at different magnifications.

3.4 Surface composition

In order to explore the chemical composition of the Cu₂O films, an ex situ XPS analysis was performed on both bare and etched surfaces of Cu₂O films prepared on stainless steel. Figure 6a presents the entire spectrum and Table ESI S2 lists the elemental contents for the prepared samples. Based on the XPS results, the Cu:O atomic ratio of 95 nm etched layer was estimated to be about 2:1, which is consistent with the form of Cu₂O obtained with XRD analysis. Besides the presence of copper and oxygen, carbon was also found on the surfaces of the prepared samples (see Fig. ESI S1-S3). After 95 nm etching, the content of C 1s that mainly comes from ambient air or the decomposition of the precursor is negligible.

As exhibited in Fig. 6b, the Cu 2p_{1/2} peak is centered at 952.25 eV and the Cu 2p_{3/2} peaks at 932.35 eV.³⁰ Since Cu 2p can hardly differentiate Cu²⁺ from Cu¹⁺, it is necessary to involve analysis of auger spectrum. The Cu auger spectrum of the obtained thin film was shown in Fig. 7a. The obvious peak located at 916.80 eV is perfectly coinciding with the standard auger spectrum of Cu₂O,

which further confirm the purity of Cu₂O synthesized in this study. The binding energies of O 1s were observed to be 529.65 and 531.45 eV (see Fig. 7b), corresponding to the lattice oxygen (O_L) and adsorbed oxygen (O_{ads}), respectively. The fitted profiles agree well with the measured profiles, as shown in Fig. 7b.

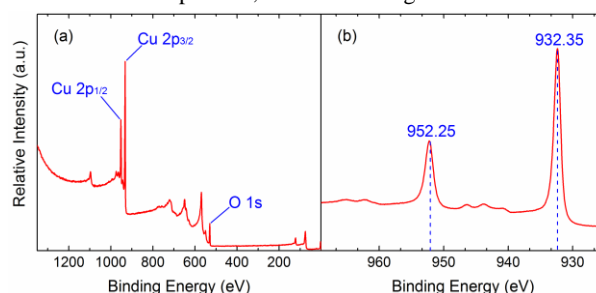


Fig. 6 Entire XPS spectrum (a) and Cu 2p spectrum (b) of Cu₂O thin film.

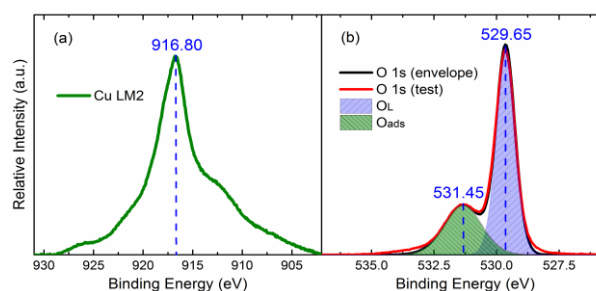


Fig. 7 Cu LM2 (a) and O 1s signals (b) of a representative Cu₂O thin film.

3.5 Catalytic performance

The catalytic performance of the Cu₂O grown on mesh of stainless steel was tested for the complete oxidation of C₂H₂ and C₃H₆ at atmospheric pressure. The background effect of the stainless steel element on the oxidation was examined by carrying out the experiments on non-coated mesh (NCM) under the same conditions. The catalytic tests were carried out three times for the same sample and the results are quite close, demonstrating that the prepared Cu₂O has good reusability with reproduced results. Figure 8 compares the temperature-dependent conversion ratio of C₂H₂ and C₃H₆ with Cu₂O-coated mesh and non-coated mesh. Compared to the non-coated mesh condition, the complete oxidation of C₂H₂ decreased from 450 to 300 °C and for C₃H₆ decreased from 675 to 425 °C over Cu₂O. It should be mentioned that during the oxidation of C₂H₂ and C₃H₆ over Cu₂O-coated mesh, CO was not detected. However, a number of CO was measured over non-coated mesh. Compared to other TMOs such as Mn₃O₄,²³ Co₃O₄,²² and Co-Mn oxides³¹ for the oxidation of C₂H₂ and C₃H₆, Cu₂O exhibits better catalytic performances.

With an Arrhenius expression,¹⁴ apparent activation energies (E_{appa}) of less than 15% of C₂H₂ and C₃H₆ conversion were deduced. The E_{appa} of C₂H₂ and C₃H₆ oxidation over non-coated mesh are 93.5 and 92.0 kJ/mol, while these values shift to 51.7 and 57.0 kJ/mol with Cu₂O-coated samples (average values for three time respectively). Compared to E_{appa} obtained with other TMOs, such as Co₃O₄ (128.9 kJ/mol for C₂H₂, 127.1 kJ/mol for C₃H₆)¹⁴ and Mn₃O₄ (84.7 kJ/mol for C₃H₆),²³ the reaction with Cu₂O shows lower E_{appa}. The abundant hollows revealed by the SEM images are expected to absorb more oxygen and reduce the activation barrier. Moreover, the high Cu:O ratio on the surfaces of the prepared samples could provide more active sites. Thus, the relatively low E_{appa} may

contribute to accelerate the oxidation processes and enhance the catalytic performance for oxidation of C_2H_2 and C_3H_6 .

It is generally accepted that the oxidation of low-rank hydrocarbons over TMOs follows the redox mechanism.³⁰ Firstly, Cu_2O reacts with oxygen, giving rise to CuO . Secondly, the reaction of C_2H_2 and C_3H_6 with the trapped or lattice oxygen occurs, leading to CuO reduction and release of oxygen to form Cu_2O . From the XPS results, both O_L and O_{ads} contain mainly O_2^{2-} and O^- species. Both O_2^{2-} and O^- are strongly electrophilic reactants. They can attack an organic molecule in the region of its highest electron density and result in the oxidation of the carbon skeleton. As the electrophilic oxygen species such as O_L and O_{ads} are generally responsible for the total oxidation of hydrocarbons to CO_2 , these electrophilic oxygen species (O_2^{2-} or O^-) presented at the surface of Cu_2O are expected to benefit for the complete conversion of C_2H_2 and C_3H_6 (see Fig. ESI S4).³² Moreover, the hollow ball-like morphology revealed by the microstructure analysis could expose more surface area and adsorb more oxygen, which would make the oxidation occur at relatively low temperatures.

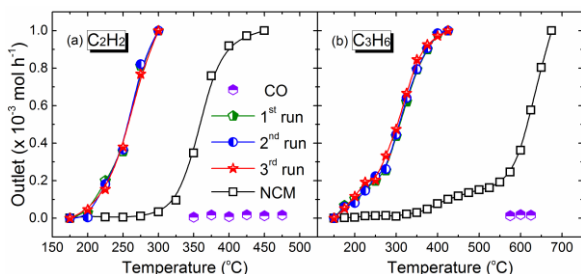


Fig. 8 Outlet profiles of C_2H_2 and C_3H_6 oxidation over NCM and mesh grid of stainless steel coated with Cu_2O .

4. Conclusions

This work presents a detailed introduction of facile synthesis of Cu_2O thin films by using a home-made PSE-CVD system for catalytic oxidation of C_2H_2 and C_3H_6 . XRD, SEM and XPS were employed to characterize the physicochemical properties of the deposited films. The catalytic oxidation of C_2H_2 and C_3H_6 over Cu_2O samples was tested at atmospheric pressure in a fixed-bed quartz reactor. XRD analysis indicates that the prepared films are pure Cu_2O . The results show that the Cu_2O leads the complete oxidation decreased by 175 °C for C_2H_2 and 250 °C for C_3H_6 relative to the non-coated mesh. According to the microstructure and XPS results, the lattice and adsorbed oxygen as well as the hollow ball-like geometry could benefit for the deep oxidation of C_2H_2 and C_3H_6 . These results reveal that Cu_2O can be easily prepared and show good potential in the catalytic abatement of VOCs.

Acknowledgements

Prof. ZYT thanks the financial support from the Recruitment Program of Global Youth Experts (Grant No. Y41Z024BA1).

Notes and references

* Corresponding author. Tel/Fax: +86-10 82543184, E-mail: tianzhenyu@iet.cn.

- O. L. Olga, S. S. Yu, N. S. Valentin and I. T. Nikolai, *Nato Sci Ss Iv Ear*, 2002, 16, 243-247.
- X. K. Chen, L. L. Feng, H. L. Luo and H. M. Cheng, *Environ Sci Pollut R*, 2014, 21, 12868-12882.

- G. Y. Li, Z. Y. Zhang, H. W. Sun, J. Y. Chen, T. C. An and B. Li, *J Hazard Mater*, 2013, 250, 147-154. DOI: 10.1039/C5RA05635G
- S. C. Kim and W. G. Shim, *Appl Catal B-Environ*, 2010, 98, 180-185.
- S. Ivanova, C. Petit and V. Pitchon, *Gold Bull*, 2006, 39, 3-8.
- A. C. Gluhoi, N. Bogdanchikova and B. E. Nieuwenhuys, *J Catal*, 2005, 232, 96-101.
- T. Maillot, C. Solleau, J. Barbier-Jr and D. Duprez, *Appl Catal B-Environ*, 1997, 14, 85-95.
- H. H. Chen, Y. Yan, Y. Shao and H. P. Zhang, *Rsc Adv*, 2014, 4, 55202-55209.
- P. Yang, S. S. Yang, Z. N. Shi, Z. H. Meng and R. X. Zhou, *Appl Catal B-Environ*, 2015, 162, 227-235.
- M. H. Khedr, K. S. A. Halim, M. I. Nasr and A. M. El-Mansy, *Mat Sci Eng a-Struct*, 2006, 430, 40-45.
- S. Somekawa, T. Hagiwara, K. Fujii, M. Kojima, T. Shinoda, K. Takane and K. Domen, *Appl Catal a-Gen*, 2011, 409, 209-214.
- A. Urbutis and S. Kitrys, *Chemija*, 2013, 24, 111-117.
- S. R. Wang, H. X. Zhang, Y. S. Wang, L. W. Wang and Z. Gong, *Rsc Adv*, 2014, 4, 369-373.
- Z. Y. Tian, N. Bahlawane, F. Qi and K. Kohse-Höinghaus, *Catal Commun*, 2009, 11, 118-122.
- S. C. Kim and W. G. Shim, *Appl Catal B-Environ*, 2008, 79, 149-156.
- R. Rostami and A. J. Jafari, *J Environ Health Sci*, 2014, 12, 1-10.
- P. Mallick, *Proceedings of the National Academy of Sciences India Section A-Physical Sciences*, 2014, 84, 387-389.
- M. Ali, F. Yehya, A. K. Chaudhary and V. V. S. S. Srikanth, *Conference on Light and Its Interactions with Matter*, 2014, 1620, 327-331.
- M. Ali, N. K. Rotte and V. V. S. S. Srikanth, *Mater Lett*, 2014, 128, 253-255.
- F. Hu, K. C. Chan, T. M. Yue and C. Surya, *Thin Solid Films*, 2014, 550, 17-21.
- J. P. Zhang and L. P. Yu, *Journal of Materials Science-Materials in Electronics*, 2014, 25, 5646-5651.
- P. Mountapmbeme Kouotou, Z. Y. Tian, U. Mundloch, N. Bahlawane and K. Kohse-Höinghaus, *Rsc Adv*, 2012, 2, 10809-10812.
- Z. Y. Tian, P. Mountapmbeme Kouotou, N. Bahlawane and P. H. Tchoua Ngamou, *J Phys Chem C*, 2013, 117, 6218-6224.
- M. C. Biesinger, L. W. M. Lau, A. R. Gerson and R. S. C. Smart, *Applied Surface Science*, 2010, 257, 887-898.
- Z. Y. Tian, H. J. Herrenbruck, P. Mountapmbeme Kouotou, H. Vieker, A. Beyer, A. Golzhauser and K. Kohse-Höinghaus, *Surf Coat Tech*, 2013, 230, 33-38.
- J. M. Valtierra, J. Ram íez-Ortiz, V. M. Arroyo-Rojas and F. Ruiz, *Applied Catalysis A*, 2003, 238, 1-9.
- G. G. Condorelli, G. Malandrino and I. Fragala, *Chem Mater*, 1994, 6, 1861-1866.
- Z. Y. Tian, N. Bahlawane, V. Vannier and K. Kohse-Höinghaus, *P Combust Inst*, 2013, 34, 2261-2268.
- X. J. Yu, Y. C. Wei, L. Z. Huang, J. F. Niu, J. Zhang, X. M. Li and B. H. Yao, *Mater Chem Phys*, 2014, 148, 727-733.
- X. S. Jiang, M. Zhang, S. W. Shi, G. He, X. P. Song and Z. Q. Sun, *J Electrochem Soc*, 2014, 161, D640-D643.
- Z. Y. Tian, P. H. Tchoua Ngamou, V. Vannier, K. Kohse-Höinghaus and N. Bahlawane, *Appl Catal B-Environ*, 2012, 117, 125-134.
- P. Mountapmbeme Kouotou, H. Vieker, Z. Y. Tian, P. H. Tchoua Ngamou, A. El Kasmi, A. Beyer, A. Golzhauser and K. Kohse-Höinghaus, *Catal Sci Technol*, 2014, 4, 3359-3367.